

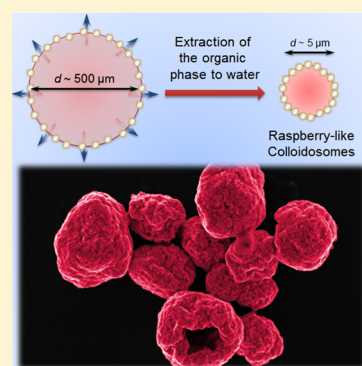
Gold Raspberry-Like Colloidosomes Prepared at the Water–Nitromethane Interface

Evgeny Smirnov,¹ Pekka Peljo,¹ and Hubert H. Girault^{1*}

Laboratoire d'Electrochimie Physique et Analytique, Ecole Polytechnique Fédérale de Lausanne, Rue de l'Industrie 17, CH-1951 Sion, Switzerland

Supporting Information

ABSTRACT: In this study, we propose a simple shake-flask method to produce micron-size colloidosomes from a liquid–liquid interface functionalized with a gold nanoparticle (AuNP) film. A step-by-step extraction process of an organic phase partially miscible with water led to the formation of raspberry-like structures covered and protected by a gold nanofilm. The distinctive feature of the prepared colloidosomes is a very thin shell consisting of small AuNPs of 12 or 38 nm in diameter instead of several hundred nanometers reported previously. The interesting and remarkable property of the proposed approach is their reversibility: the colloidosomes may be easily transformed back to a nanofilm state simply by adding pure organic solvent. The obtained colloidosomes have a broadband absorbance spectrum, which makes them of great interest in applications such as photothermal therapy, surface-enhanced Raman spectroscopy studies, and microreactor vesicles for interfacial electrocatalysis.



INTRODUCTION

Colloidosomes were introduced in 2002 as microcontainers similar to vesicles but obtained in Pickering emulsions, i.e., emulsions stabilized by solid particles.¹ Because they have attracted great interest,^{2–9} their possible applications ranged from drug delivery⁴ and photothermal therapy systems⁷ to effective light absorbers based on the so-called “black gold”⁶ and surface-enhanced Raman spectroscopy (SERS) platform because of the concentration of analyte molecules and small interparticle distances between separate nanoparticles in a colloidosome.^{8,9}

Usually, the preparation of colloidosomes takes place by the self-assembly of nano or microparticles at an interface of two immiscible or partially miscible liquids, followed by the formation and stabilization of the colloids after vigorous shaking. Such liquid–liquid systems may consist of water and oil, where self-assembly and stabilization occurs by the reduction of the interfacial energy due to the adsorption of nanoparticles^{1,3,4} or at the interface of water-in-water emulsions by using aqueous phase-separated polymer solutions.² The assembly process at the liquid–liquid interface has several advantages: defect-free pristine nature (facilitating reproducibility), self-healing and self-restoring properties (allowing correction of assembly errors), mechanical plasticity (can be deformed in any direction), and possibility to create both 2D and 3D structures.^{10–13} The latter allowed the implementation of electrochemically driven self-assembly at liquid–liquid interfaces.¹⁴ The topic of particle self-assembly at various fluid–fluid interfaces has been recently reviewed by Binks.¹⁵

Very recently, water–oil systems with low interfacial tension, such as water–nitromethane (MeNO₂)¹³ and water–propylene carbonate,¹⁶ have been shown to facilitate gold nanoparticle

(AuNP) assembly at a liquid–liquid interface. The combination of these latest works with the previous studies on tetrathiafulvalene (TTF)-promoted self-assembly of citrate-covered AuNPs (citrate@AuNPs)¹² have been used here to produce colloidosomes. In a nut shell, TTF undergoes oxidation to TTF⁺ on the surface of AuNPs. Because of the strong affinity between gold and sulfur atoms in TTF and TTF⁺ molecules, citrate is substituted as the ligand on the nanoparticle surface with TTF. At the same time, π – π interactions between TTF and TTF⁺ provide a force that keeps neighboring nanoparticles together within the film, preventing irreversible aggregation. Therefore, the use of TTF–AuNP nanofilms is promising for colloidosome preparation.

Herein, we describe a simple way to produce colloidosomes with a size ranging from submicron ($\sim 0.5 \mu\text{m}$) up to $20 \mu\text{m}$ decorated with AuNPs in a raspberry-like manner. These raspberry colloidosomes are formed with a shake-flask method from citrate@AuNPs and do not require complex functionalization of AuNPs.

EXPERIMENTAL METHODS

Chemicals. Tetrachloroauric acid (HAuCl₄, 99.9%) and TTF were received from Aldrich. Citrate trisodium dihydrate (Na₃C₆H₅O₇·2H₂O) was purchased from Fluka. Silver nitrate (AgNO₃) was bought from Chempur and ascorbic acid (C₆H₈O₆) from Riedel-de-Haën. MeNO₂ was purchased from Sigma-Aldrich. All chemicals were used as received without further purification. In all experiments, Millipore water (18.2 M Ω cm) was used.

Received: October 10, 2017

Revised: January 12, 2018

Published: January 27, 2018

Synthesis of AuNPs and Their Characterization. Suspensions of AuNPs with various mean diameters were prepared using the seed-mediated growth method.¹⁷ Seed particles for this method were synthesized by a commonly used Turkevich method.^{18,19} Details on the procedure are given in ref 13.

The obtained colloidal solutions of AuNPs were characterized by UV–vis–nearIR spectroscopy using a standard Cary 8453 (Agilent) spectrophotometer with a 10 mm quartz cell. Also, all other UV–vis–nearIR measurements were carried out with this equipment. UV–vis–nearIR spectra were recorded in total transmittance (or extinction conditions). As we cannot differentiate between the absorbed and the scattered light by the colloidosomes, the transmission spectra were converted to the extinction spectra as follows: $E_x = -\log_{10} T$, where T is the transmittance of light through the cuvette. The background signal of water was subtracted from all the recorded spectra. The measured extinction is given in arbitrary units (a.u.).

Mean diameter and concentration of nanoparticles in the prepared solution were determined as described by Haiss and co-workers²⁰ based on the absorbance spectrum and were equal to 2×10^9 particles μL^{-1} for 12 nm particles and 3×10^8 particles μL^{-1} for 38 nm particles, respectively. According to TEM investigation the mean particle sizes and distributions were 12 ± 1 and 35 ± 5 nm. Details on all necessary calculations are given in refs 11 and 20.

Scanning electron microscopy (SEM) images were recorded using Merlyn (Zeiss, Germany) or Teneo (FEI, Czech Republic) microscopes equipped with a field emission electron source (so-called, FE-SEM) operating at 3–5 kV with secondary electron (SE2) or InLens detectors. Energy-dispersive X-ray spectroscopy (EDX) was acquired with a silicon drift detector X-Max 80 (Oxford Instruments, UK) installed in a Merlyn microscope and by using INCA software package.

Confocal fluorescence images were recorded by a confocal laser scanning microscopy technique on a laser scanning confocal microscope (LSM 510, Zeiss). This microscope was operated at the laser excitation wavelength of 458 nm and 10% of the maximal intensity with the low-pass filter at 470 nm (LP 470), the pinhole was 600 μm . Fluorescent Coumarin 314 dye was chosen as the only oil-soluble dye, which can be excited with the selected wavelength. This dye was used to visually separate oil droplets from the water medium. The concentration of the dye was as low as 1 μM in the initial 1 mL droplet of MeNO_2 .

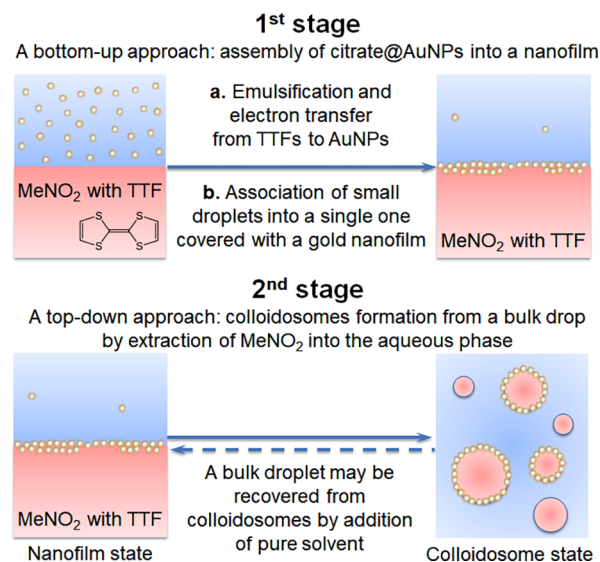
RESULTS AND DISCUSSION

Raspberry-Like Colloidosome Formation. The first stage of the colloidosome preparation process was the formation of a AuNP film or a nanofilm adsorbed at a liquid–liquid interface. As shown previously, a nanofilm can be prepared at interfaces of high interfacial tension, such as water–1,2-dichloroethane, in the presence of TTF.¹² The role of TTF in this process is reducing the charge of AuNPs and preventing irreversible nanoparticle aggregation due to π – π -bonding between TTF molecules attached to the gold surface. The same strategy was recently applied to prepare nanofilms at the MeNO_2 –water interface.¹³

The second stage included the addition of water to extract the organic solvent that is partially miscible with water. Because of the relatively high solubility of MeNO_2 in water, this extraction process decreased rapidly the volume of the organic phase, finally leading to disintegration of the organic phase into small droplets covered with AuNPs. This process is schematically represented in Scheme 1.

As MeNO_2 solubility in water was reported to be between 10 and 12 wt %, ^{21,22} 1 mL MeNO_2 can be fully extracted to the aqueous phase by ca. 9.5 mL of water. This process was carried out in a step-by-step manner to highlight the volume changes of the organic phase during this stage (Figure 1A). At the first step, 4 mL of aqueous citrate@AuNPs with a mean diameter of 38 nm was added to 1 mL of 1 mM TTF solution in MeNO_2

Scheme 1. Schematic Representation of the Colloidosome Formation Based on the Two Step Process^a



^aAt the first stage, AuNPs form a nanofilm on a macroscopic droplet of the organic phase. At the second stage, subsequent extraction leads to one droplet to break apart into many micron-sized colloidosomes.

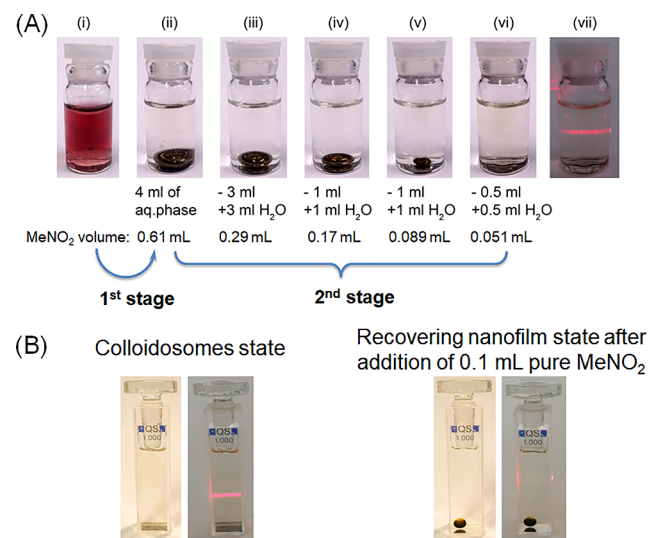


Figure 1. Colloidosome formation by subsequent extraction of the organic solvent to water and shrinking droplet covered by a nanofilm of AuNPs. (A) Step-by-step formation of colloidosomes from a bulk MeNO_2 droplet covered with a hexagonal close-packed monolayer of 38 nm AuNPs by a subsequent extraction process. (i) Initial solution mixture of two liquids (AuNPs at the top, MeNO_2 with TTF at the bottom). (ii–vi) Subsequent shrinking of the MeNO_2 droplet volume. Numbers under each photo represent removed (“–”) and added (“+”) amount of water. Also, the calculated volumes of the remaining MeNO_2 droplets are given for each picture. (vi,vii) Formed colloidosomes are visible only by the scattering of a laser beam. (B) A full recovery to a nanofilm state from colloidosomes after the addition of 0.1 mL of pure MeNO_2 solvent.

(Figure 1A(i)). The flask was vigorously shaken and the suspension was left to settle into a single drop of the organic phase covered by a nanofilm (Figure 1A(ii)). Then, the top aqueous phase was substituted with fresh water, vigorously shaken, and left to settle. The repetition of the step for several

times leads to significant reduction of the organic phase volume (Figure 1A(iii)–(v)). Figure 1A also depicts volumes of removed solution, added water, and remaining MeNO₂ in the droplet at each step. The latter was calculated by taking into account the values for solubility of MeNO₂ in water as 10.4 wt % and water in MeNO₂ as 1.6 wt %, ²¹ and assuming the densities of MeNO₂ saturated water as 1.002 g/mL and water saturated MeNO₂ as 1.130 g/mL (molar fraction weighted average of the densities of the pure compounds at 20 °C). At the end, when colloidosomes were formed, the MeNO₂ droplet disappeared forming a new “invisible” for a naked eye colloid solution (Figure 1A(vi)), whose presence can be visualized by Tyndall scattering (Figure 1A(vii)). To obtain colloidosomes from 12 nm AuNPs with the same surface coverage as that from 38 nm AuNPs, at the first step, only 1 mL of the initial 12 nm AuNP solution was used and another 3 mL of pure water was added.

Interestingly, the colloidosomes obtained with the present procedure possess a remarkable property. Thus, colloidosomes may be fully recovered back to the initial nanofilm state after the addition of a small volume (100 μL) of pure MeNO₂ solution (Figure 1B). As reported in several papers, ^{12,13,16} the formation of a nanofilm here involves charging of AuNPs by TTF molecules and substitution of citrate ligands to form TTF-covered AuNPs (TTF@AuNPs). During this process part of TTF⁺, TTF₂⁺, and other charge-shared complexes of TTF are easily partitioned to and stay in the aqueous phase. TTF also plays an important role in linking the nanoparticles together in the nanofilm and giving the freedom for nanoparticles to slide relative to each other upon shaking, because of the unique π – π interactions between the TTF molecules. ¹³ The latter provides the so-called self-healing nature of a nanofilm consisting of TTF@AuNPs and allows the nanoparticle film rearrangement upon shaking or ultrasonication. ¹³

Arrangement of Gold Nanoparticles on the Surface of Colloidosomes. Upon complete extraction of the organic solvent to the aqueous phase, both colloidosomes and solid particles of a compound originally dissolved in the organic phase (like TTF) may be formed, depending on the conditions. We prepared SEM samples of colloidosomes and investigated the morphology and arrangement of the AuNPs in the nanofilm on the surface of colloidosomes (Figure 2). Colloidosomes of two AuNPs of diameters 12 and 38 nm were prepared with higher TTF concentration (2 mM instead of 1 mM) to form a solid TTF support for a thin and brittle nanofilm.

SEM investigation showed that colloidosomes were covered with densely packed islands of a single nanoparticle thickness in both cases. Some of these islands were fully immersed (“sunk”) in the TTF matrix during the drying process by capillary forces (Figure 2A). Oppositely, if the TTF amount is reduced down to 10 μM, hollow shells consisting of nanoparticles were observed (Figure 2B). Such hollow shells collapsed upon SEM sample preparation, highlighting that TTF is essential to act as a binder and support for the fragile films when the solvent is removed. Finally, in the absence of AuNPs, solid particles of TTF could be prepared, as described below.

This feature of a single particle thickness for the present TTF system and the small size of the used AuNPs are unique and different from previously reported methods on AuNP assembly. For instance, the slow extraction process that leads to nanoparticle macrostructures ²³ or multilayer rigid shells of larger nanoparticles in the case of butanol–water system ⁶ or octanol–water system. ²⁴ Notably, thin films of a small size

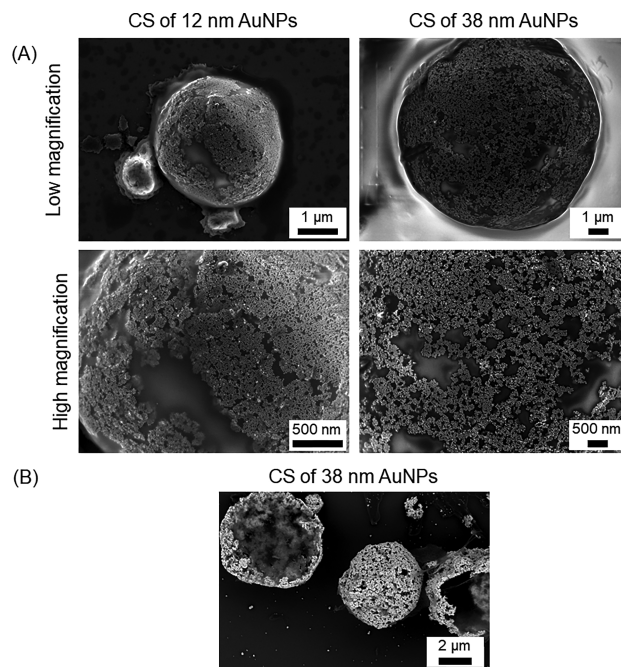


Figure 2. Morphology of colloidosomes (CS) obtained after the extraction process at the water–MeNO₂ interface. (A) Colloidosomes formed with AuNPs of two mean diameters 12 and 38 nm and larger TTF concentration (2 mM) to visualize the nanofilm structure at the surface. (B) Colloidosomes prepared with 38 nm AuNPs and low TTF content (10 μM) with a hollow shell structure.

(below 10 nm) consisting of Fe₃O₄ nanoparticles or CdTe quantum dots functionalized with interfacial stabilizing agents were previously obtained and used to form colloidosomes. ³

Surprisingly, SEM studies revealed that some solid spherical particles were not covered by AuNPs at all. Further chemical analysis with EDX confirmed that these bare particles consisted of TTF because of the presence of sulfur and the absence of gold atoms (Figure S1 in the Supporting Information). Oppositely, data recorded from colloidosomal area contained both sulfur and gold in considerable amounts. Thus, under extraction conditions TTF molecules solidified in TTF spheres rather than a more typical rod-like morphology, ^{25–27} when the extraction of the organic phase to water was completed. This happened because of very low solubility of TTF in the water phase and confinement conditions from the interface between water and MeNO₂. Finally, the formation of TTF spheres without a nanofilm can be explained by insufficient interfacial concentration of AuNPs in comparison with largely increased surface area upon transformation of macroscopic droplets into colloidosomes. Additionally, this shows that the same technique can be used to prepare micron-sized particles of any material soluble in the organic phase but insoluble in the aqueous phase.

Optical Properties of Raspberry-Like Colloidosomes. Figure 3A shows optical properties of the obtained colloidosomes made of 12 and 38 nm AuNPs. The UV–vis spectra (straight blue and orange lines) are significantly different from the spectra of the initial solutions (dotted lines of the same colors). Instead of the distinguishable plasmon peaks, as for example, in the case of a gold nanofilm, ¹³ we observed a continuous absorption over the entire range of wavelengths (from 400 to 1100 nm). Most likely, the multiplicity of the obtained colloidosome diameters leads to heavily overlapped spectra of individual-sized colloidosomes,

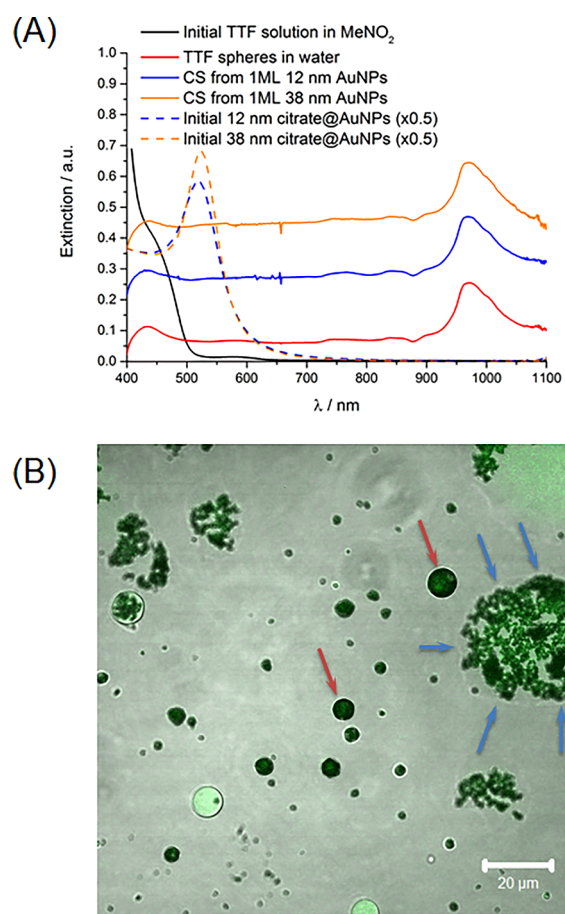


Figure 3. Optical properties of colloidosomes (CS) prepared from one hexagonal close-packed monolayer of 12 and 38 nm AuNPs. (A) Comparison of UV-vis-NIR spectra of colloidosome solution right after the formation and initial spectra of citrate@AuNPs. (B) Confocal fluorescence microscopy of colloidosomes made from 38 nm AuNPs shows fully formed (red arrows) and not completely (blue arrows) formed colloidosomes. Scale bar is 20 μ m.

and therefore, the solution has a dark color. The latter is clearly demonstrated by confocal fluorescence microscopy observations (Figure 3B). Fully (red arrow) and not completely (blue arrow) formed colloidosomes were present at the same time, and they had size ranging from ca. 2 to 20 μ m, whereas according to electron microscopy investigation their size may be down to 0.5 μ m in a dry state. Also, on the basis of confocal images we calculated the mean diameter of the colloidosomes, which equals to 4 ± 2 and 4.2 ± 1.5 μ m in the cases of 12 and 38 nm AuNPs, respectively. A detailed description of a confocal microscopy study, images of each channel, and statistical distribution of the colloidosome diameter are given in section 2 of the Supporting Information.

Also, we carried out a blank experiment, where only bare TTF spheres were obtained in the absence AuNPs (red line in Figure 3A). These TTF spheres display some extinction of light, but the addition of AuNPs significantly reduces the transmission of light through the sample, and this effect is enhanced for larger NPs. Nevertheless, the presence of TTF molecules has a minor effect on the UV-vis spectra of colloidosomes as the extinction is three to five times smaller than that for AuNP-containing colloidosomes. Furthermore, we carried out UV-vis-NIR measurements of TTF in MeNO₂ and TTF⁺ in water obtained by the extraction of ions to the

aqueous phase from MeNO₂ (section 3 of Supporting Information), which showed that both TTF and TTF⁺ in the form of solutions did not have strong absorbance around 1000 nm. According to these two experiments, the appearance of the peak at \sim 1000 nm, when the particles are formed, is not fully understood and requires further investigation.

Finally, we propose a route to avoid the formation or minimize the amount of such empty TTF spheres and increase the colloidosome formation. We increased the initial concentration of AuNPs in the nanofilm by five times. Figure 4A demonstrates experiments with one hexagonal close-packed

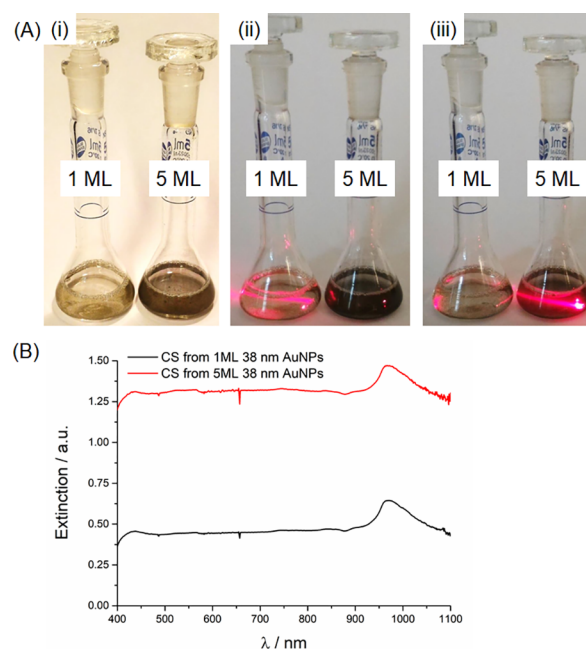


Figure 4. Significant increase of colloidosome (CS) color intensity with increasing AuNPs content by five times. (A) (i) Photo of two flasks: the left one contains colloidosomes obtained from a nanofilm with AuNP coverage of ca. one monolayer, the right one contains colloidosomes obtained from a nanofilm of five AuNP monolayers. (ii,iii) Photos of two flasks show Tyndall scattering from colloidosomes with dimmed ambient light. (B) Corresponding UV-vis spectra of the colloidosomes obtained with 1 and 5 ML of AuNP coverage.

monolayer of nanoparticles and five monolayers of 38 nm AuNPs. In the case of higher nanoparticle loading, the final solution of colloidosomes looked denser and significantly darker than the diluted one (lesser AuNP content). The latter was confirmed by recording the UV-vis spectra from the obtained samples, showing minimal transmission of light through the sample (Figure 4B).

CONCLUSIONS

In summary, we have developed a simple and facile shake-flask approach to obtain colloidosomes covered by AuNPs, ranging from 0.5 to 20 μ m. The latter was achieved by the extraction of the organic phase partially soluble in water that led to a significant decrease of the organic phase volume and eventual disintegration of the droplet to form micrometer-sized colloids. The remarkable property of the present approach is its reversibility: the obtained colloidosomes were easily changed from colloidosomes back to the nanofilm state by adding a pure organic solvent. Combined with the previous works on redox

electrocatalysis,^{28–30} it opens novel opportunities to use such colloidosomes as a biphasic microreactor platform for redox reactions between redox couples in both phases with ion and electron permittivity across the nanofilm. For example, when used as microreactors, these colloidosomes may be turned back into a single bulk droplet for convenient analyses. Besides that the obtained colloidosomes showed a broadband absorbance spectrum and linked with the present relatively easy ways to form colloidosomes may be of interest in applications such as SERS and photothermal therapy. Finally, the present approach may be used to concentrate organic soluble compounds (e.g., with a similar approach used in ref 31) and to obtain spherical solid particles of molecules soluble in the organic phase and insoluble in water because of the interfacial confinement, as we have demonstrated for TTF.

■ ASSOCIATED CONTENT

Supporting Information

The Supporting Information is available free of charge on the ACS Publications website at DOI: [10.1021/acs.langmuir.7b03532](https://doi.org/10.1021/acs.langmuir.7b03532).

EDX investigation of colloidosomes, details on confocal microscopy studies, colloidosome size distribution, UV-Vis spectra of TTF and TTF⁺ (PDF)

■ AUTHOR INFORMATION

Corresponding Author

*E-mail: Hubert.Girault@epfl.ch. Fax: (+)41 (0)21 693 36 67. Homepage: lepa.epfl.ch.

ORCID

Evgeny Smirnov: [0000-0001-7930-7758](https://orcid.org/0000-0001-7930-7758)

Pekka Peljo: [0000-0002-1229-2261](https://orcid.org/0000-0002-1229-2261)

Hubert H. Girault: [0000-0001-5573-5774](https://orcid.org/0000-0001-5573-5774)

Author Contributions

The manuscript was written through contributions of all authors. All authors have given approval to the final version of the manuscript.

Funding

We would like to acknowledge financial support from Swiss National Science Foundation, Ambizione Energy, grant 160553 and EPFL.

Notes

The authors declare no competing financial interest.

■ ACKNOWLEDGMENTS

Authors acknowledge help of Samuel Terretaz (LCPPM, EPFL) with confocal fluorescence microscopy.

■ ABBREVIATIONS

TTF, tetrathiafulvalene; MeNO₂, nitromethane; SERS, surface-enhanced Raman spectroscopy; AuNP, gold nanoparticle; SEM, scanning electron microscopy; EDX, energy-dispersive X-ray spectroscopy; CS, colloidosomes.

■ REFERENCES

(1) Dinsmore, A. D.; Hsu, M. F.; Nikolaidis, M. G.; Marquez, M.; Bausch, A. R.; Weitz, D. A. Colloidosomes: Selectively Permeable Capsules Composed of Colloidal Particles. *Science* **2002**, *298*, 1006–1009.

(2) Poortinga, A. T. Microcapsules from Self-Assembled Colloidal Particles Using Aqueous Phase-Separated Polymer Solutions. *Langmuir* **2008**, *24*, 1644–1647.

(3) Duan, H.; Wang, D.; Sobal, N. S.; Giersig, M.; Kurth, D. G.; Möhwald, H. Magnetic Colloidosomes Derived from Nanoparticle Interfacial Self-Assembly. *Nano Lett.* **2005**, *5*, 949–952.

(4) Yang, X.-C.; Samanta, B.; Agasti, S. S.; Jeong, Y.; Zhu, Z.-J.; Rana, S.; Miranda, O. R.; Rotello, V. M. Drug Delivery Using Nanoparticle-Stabilized Nanocapsules. *Angew. Chem., Int. Ed.* **2011**, *50*, 477–481.

(5) Xu, X.-W.; Zhang, X.-M.; Liu, C.; Yang, Y.-L.; Liu, J.-W.; Cong, H.-P.; Dong, C.-H.; Ren, X.-F.; Yu, S.-H. One-Pot Colloidal Chemistry Route to Homogeneous and Doped Colloidosomes. *J. Am. Chem. Soc.* **2013**, *135*, 12928–12931.

(6) Liu, D.; Zhou, F.; Li, C.; Zhang, T.; Zhang, H.; Cai, W.; Li, Y. Black Gold: Plasmonic Colloidosomes with Broadband Absorption Self-Assembled from Monodispersed Gold Nanospheres by Using a Reverse Emulsion System. *Angew. Chem., Int. Ed.* **2015**, *54*, 9596–9600.

(7) Huang, P.; Lin, J.; Li, W.; Rong, P.; Wang, Z.; Wang, S.; Wang, X.; Sun, X.; Aronova, M.; Niu, G.; Leapman, R. D.; Nie, Z.; Chen, X. Biodegradable Gold Nanovesicles with an Ultrastrong Plasmonic Coupling Effect for Photoacoustic Imaging and Photothermal Therapy. *Angew. Chem., Int. Ed.* **2013**, *52*, 13958–13964.

(8) Phan-Quang, G. C.; Lee, H. K.; Phang, I. Y.; Ling, X. Y. Plasmonic Colloidosomes as Three-Dimensional SERS Platforms with Enhanced Surface Area for Multiphase Sub-Microliter Toxin Sensing. *Angew. Chem., Int. Ed.* **2015**, *54*, 9691–9695.

(9) Turek, V. A.; Francescato, Y.; Cadinu, P.; Crick, C. R.; Elliott, L.; Chen, Y.; Urand, V.; Ivanov, A. P.; Velleman, L.; Hong, M.; Vilar, R.; Maier, S. A.; Giannini, V.; Edel, J. B. Self-Assembled Spherical Supercluster Metamaterials from Nanoscale Building Blocks. *ACS Photonics* **2016**, *3*, 35–42.

(10) Wang, D.; Duan, H.; Möhwald, H. The Water/oil Interface: The Emerging Horizon for Self-Assembly of Nanoparticles. *Soft Matter* **2005**, *1*, 412–416.

(11) Binks, B. P. Particles as Surfactants—similarities and Differences. *Curr. Opin. Colloid Interface Sci.* **2002**, *7*, 21–41.

(12) Smirnov, E.; Scanlon, M. D.; Momotenko, D.; Vrabel, H.; Méndez, M. A.; Brevet, P.-F.; Girault, H. H. Gold Metal Liquid-Like Droplets. *ACS Nano* **2014**, *8*, 9471–9481.

(13) Smirnov, E.; Peljo, P.; Scanlon, M. D.; Gumy, F.; Girault, H. H. Self-Healing Gold Mirrors and Filters at Liquid–liquid Interfaces. *Nanoscale* **2016**, *8*, 7723–7737.

(14) Montelongo, Y.; Sikdar, D.; Ma, Y.; McIntosh, A. J. S.; Velleman, L.; Kucernak, A. R.; Edel, J. B.; Kornyshev, A. A. Electrotunable Nanoplasmonic Liquid Mirror. *Nat. Mater.* **2017**, *16*, 1127–1135.

(15) Binks, B. P. Colloidal Particles at a Range of Fluid–Fluid Interfaces. *Langmuir* **2017**, *33*, 6947–6963.

(16) Smirnov, E.; Peljo, P.; Girault, H. H. Self-Assembly and Redox Induced Phase Transfer of Gold Nanoparticles at a Water–propylene Carbonate Interface. *Chem. Commun.* **2017**, *53*, 4108–4111.

(17) Park, Y.-K.; Yoo, S.-H.; Park, S. Assembly of Highly Ordered Nanoparticle Monolayers at a Water/hexane Interface. *Langmuir* **2007**, *23*, 10505–10510.

(18) Turkevich, J.; Stevenson, P. C.; Hillier, J. A Study of the Nucleation and Growth Processes in the Synthesis of Colloidal Gold. *Discuss. Faraday Soc.* **1951**, *11*, 55–75.

(19) Frens, G. Controlled Nucleation for the Regulation of the Particle Size in Monodisperse Gold Suspensions. *Nat. Phys. Sci.* **1973**, *241*, 20–22.

(20) Haiss, W.; Thanh, N. T. K.; Aveyard, J.; Fernig, D. G. Determination of Size and Concentration of Gold Nanoparticles from UV–Vis Spectra. *Anal. Chem.* **2007**, *79*, 4215–4221.

(21) Sazonov, V. P.; Marsh, K. N.; Hefter, G. T. IUPAC-NIST Solubility Data Series 71. Nitromethane with Water or Organic Solvents: Binary Systems. *J. Phys. Chem. Ref. Data* **2000**, *29*, 1165–1354.

(22) Sazonov, V. P.; Marsh, K. N.; Shaw, D. G.; Chernysheva, M. F.; Sazonov, N. V.; Akaiwa, H. IUPAC-NIST Solubility Data Series. 72. Nitromethane with Water or Organic Solvents: Ternary and Quaternary Systems. *J. Phys. Chem. Ref. Data* **2000**, *29*, 1447–1641.

(23) Zanaga, D.; Bleichrodt, F.; Altantzis, T.; Naomi Winckelmans, N.; Palenstijn, W. J.; Sijbers, J.; de Nijs, B.; van Huis, M. A.; Sanchez-Iglesias, A.; Liz-Marzan, L. M.; van Blaaderen, A.; Batenburg, K. J.; Bals, S.; Van Tendeloo, G. Quantitative 3D Analysis of Huge Nanoparticle Assemblies. *Nanoscale* **2016**, *8*, 292–299.

(24) Xiao, M.; Hu, Z.; Wang, Z.; Li, Y.; Tormo, A. D.; Le Thomas, N.; Wang, B.; Gianneschi, N. C.; Shawkey, M. D.; Dhinojwala, A. Bioinspired Bright Noniridescent Photonic Melanin Supraballs. *Sci. Adv.* **2017**, *3*, No. e1701151.

(25) Naka, K.; Ando, D.; Wang, X.; Chujo, Y. Synthesis of Organic-Metal Hybrid Nanowires by Cooperative Self-Organization of Tetrathiafulvalene and Metallic Gold via Charge-Transfer. *Langmuir* **2007**, *23*, 3450–3454.

(26) Puigmartí-Luis, J.; Schaffhauser, D.; Burg, B. R.; Dittrich, P. S. A Microfluidic Approach for the Formation of Conductive Nanowires and Hollow Hybrid Structures. *Adv. Mater.* **2010**, *22*, 2255–2259.

(27) Xing, Y.; Wyss, A.; Esser, N.; Dittrich, P. S. Label-Free Biosensors Based on in Situ Formed and Functionalized Microwires in Microfluidic Devices. *Analyst* **2015**, *140*, 7896–7901.

(28) Smirnov, E.; Peljo, P.; Scanlon, M. D.; Girault, H. H. Interfacial Redox Catalysis on Gold Nanofilms at Soft Interfaces. *ACS Nano* **2015**, *9*, 6565–6575.

(29) Peljo, P.; Manzanares, J. A.; Girault, H. H. Contact Potentials, Fermi Level Equilibration, and Surface Charging. *Langmuir* **2016**, *32*, 5765–5775.

(30) Smirnov, E.; Peljo, P.; Scanlon, M. D.; Girault, H. H. Gold Nanofilm Redox Catalysis for Oxygen Reduction at Soft Interfaces. *Electrochim. Acta* **2016**, *197*, 362–373.

(31) Cecchini, M. P.; Turek, V. A.; Paget, J.; Kornyshev, A. A.; Edel, J. B. Self-Assembled Nanoparticle Arrays for Multiphase Trace Analyte Detection. *Nat. Mater.* **2012**, *12*, 165–171.